Anal. Chem. **2009,** *81,* 790–796

Polycyclic Aromatic Hydrocarbon Analysis with the Mars Organic Analyzer Microchip Capillary Electrophoresis System

Amanda M. Stockton, Thomas N. Chiesl, James R. Scherer, and Richard A. Mathies*

Department of Chemistry, University of California, Berkeley, California 94720

The Mars Organic Analyzer (MOA), a portable microchip capillary electrophoresis (CE) instrument developed for sensitive amino acid analysis on Mars, is used to analyze laboratory standards and real-world samples for polycyclic aromatic hydrocarbons (PAHs). The microfabricated CE separation and analysis method for these hydrophobic analytes is optimized, resulting in a separation buffer consisting of 10 mM sulfobutylether-β-cyclodextrin, 40 mM methyl-β-cyclodextrin, 5 mM carbonate buffer at pH 10, 5 °C. A PAH standard consisting of seven PAHs found in extraterrestrial matter and two terrestrial PAHs is successfully baseline separated. Limits of detection for the components of the standard ranged from 2000 ppm to 6 ppb. Analysis of an environmental contamination standard from Lake Erie and of a hydrothermal vent chimney sample from the Guaymas Basin agreed with published composition. A Martian analogue sample from the Yungay Hills region of the Atacama Desert was analyzed and found to contain 9,10-diphenylanthracene, anthracene, anthanthrene, fluoranthene, perylene, and benzo[ghi]fluoranthene at ppm levels. This work establishes the viability of the MOA for detecting and analyzing PAHs in in situ planetary exploration.

The analysis of polycyclic aromatic hydrocarbons (PAHs) in terrestrial and extraterrestrial environments is particularly pertinent because of their resistance to oxidative and photochemical degradation.[1] Terrestrial PAHs are predominantly formed via the pyrolysis, dehydrogenation, and incomplete combustion of biogenic material.[1] PAHs can also be produced via abiotic reactions, both in space and through planetary geological activity.[1,2] PAHs have been found throughout the universe, specifically in carbonaceous chondrite meteorites,[3] Martian meteorites,[4−6] and interplanetary dust particles,[7] and radioastronomers have observed PAHs in interstellar matter.[2] Given these extraterrestrial PAH sources, an infall-rate of organic matter onto the Martian surface of approximately 10^5 kg per year,[8] and arguments for abiotic syntheses of PAHs directly on the Martian surface,[1] it is important to probe for PAHs in any survey for organic carbon on its surface.

The Viking landers in 1976 and 1977 probed for but did not detect any organic molecules on Mars.[9] This result led to the widely held postulate that the Martian regolith contains a strong oxidant.[10] Since Mars has no protective magnetic field and a minimal atmosphere, it has also been postulated that organic molecules on the uppermost surface of the Martian regolith have been destroyed by irradiative sterilization.[10] These concerns indicate how critical it is to improve the sensitivity of PAH detection in such planetary exploration.

Terrestrial analysis for PAHs is of interest in health and environmental studies because of the carcinogenicity of these molecules. While PAHs can be found in a number of natural geological sources including volcanic ash, hydrothermal vents,[11] coal[12] and petroleum deposits, and oil shales,[13] there are a number of anthropomorphic contributions to PAH prevalence. PAH pollution stems from auto exhaust,[14] wood and cigarette smoke,[15] lumber processing plants,[16] and so forth, leading to PAH contamination in, for example, marine environments[17] and in the air over major cities.[18] Currently, terrestrial sampling and analysis is focused on the cleanup of environmental contamination sites.[19,20] While there have been recent advances in the analysis of PAHs

* To whom correspondence should be addressed. E-mail: ramathies@berkeley.edu. Phone: 510-642-4192. Fax: 510-642-3599.

(1) Zolotov, M.; Shock, E. *J. Geophys. Res.* **1999**, *104*, 14033–14049.
(2) Herbst, E. *Angew. Chem., Int. Ed. Engl.* **1990**, *29*, 595–608.
(3) Sephton, M. A. *Nat. Prod. Rep.* **2002**, *19*, 292–311.
(4) Becker, L.; Popp, B.; Rust, T.; Bada, J. L. *Earth Planet. Sci. Lett.* **1999**, *167*, 71–79.
(5) Jull, A. J. T.; Courtney, C.; Jeffrey, D. A.; Beck, J. W. *Science* **1998**, *279*, 366–369.
(6) McKay, D. S.; Gibson, E. K.; Thomas-Keptra, K. L.; Vali, H.; Romanek, C. S.; Clemett, S. J.; Chillier, X. D. F.; Maechling, C. R.; Zare, R. N. *Science* **1996**, *273*, 924–930.
(7) Clemett, S. J.; Maechling, C. R.; Zare, R. N.; Swan, P. D.; Walker, R. M. *Science* **1993**, *262*, 721–725.
(8) Flynn, G. J. *Earth, Moon, Planets* **1996**, *72*, 469–474.
(9) Biemann, K.; Oro, J.; Toulmin, P. I.; Orgel, L. E.; Nier, A. O.; Anderson, D. M.; Simmonds, P. G.; Flory, D.; Diaz, A. V.; Rushneck, D. R.; Biller, J. A. *Science* **1976**, *194*, 72–76.
(10) Benner, S. A.; Devine, K. G.; Matveeva, L. N.; Powell, D. H. *Proc. Natl. Acad. Sci. U.S.A.* **2000**, *97*, 2425–2430.
(11) Simoneit, B. R. T.; Lein, A. Y.; Peresypkin, V. L.; Osipov, G. A. *Geochim. Cosmochim. Acta* **2004**, *68*, 2275–2294.
(12) Bobbitt, D. R.; Reitsma, B. H.; Rougvie, A.; Yeung, E. S.; Aida, T.; Chen, Y.; Smith, B. F.; Squires, T. G.; Vernier, C. G. *Fuel* **1985**, *64*, 114–118.
(13) *Oil Shale Technology*; Lee, S., Ed.; CRC Press: Boca Raton, FL, 1990.
(14) Kraft, J.; Hartung, A.; Lies, K.-H.; Schulze, J. *J. High Resolut. Chromatogr.* **1982**, *5*, 489–494.
(15) Maga, J. A. *J. Agric. Food Chem.* **1986**, *34*, 249–251.
(16) Brown, R. S.; Luong, J. H. T.; Szolar, O. H. J.; Halasz, A.; Hawari, J. *Anal. Chem.* **1996**, *68*, 287–292.
(17) Obana, H.; Hori, S.; Kashimoto, T. *Bull. Environ. Contam. Toxicol.* **1981**, *26*, 613–620.
(18) Song, G.-Q.; Peng, Z.-L.; Lin, J.-M. *J. Sep. Sci.* **2006**, *29*, 2065–2071.

10.1021/ac802033u CCC: $40.75
Published on Web 12/15/2008

from these samples including micellar electrokinetic chromatography and supercritical fluid chromatography,[19−21] reverse-phase HPLC remains one of the most commonly used methods.[21] Because of the long analysis times, high cost, and sample blending and destruction of these methods, it would be useful to have inexpensive, rapid, nondestructive, in situ techniques for the measurement of PAH contamination in sediments.[19]

The European Space Agency (ESA) has planned the ExoMars rover as a part of its Aurora program to search for evidence of past or present life on Mars via the analysis of organic molecules. While Viking was confined to a single sampling site, ExoMars will be able to transit to promising sampling sites. Furthermore, ExoMars will have drilling capability down to 2 m depth, where organics have increased survival.[22] ExoMars will carry a suite of experiments targeting organic molecules, specifically those indicative of life. In particular, ExoMars will carry the Urey instrument,[23] which utilizes subcritical water extraction and the Mars Organic Analyzer (MOA) microchip CE separation system for high sensitivity organic molecule detection.

The MOA contains the electrical, optical, and microfluidic systems required for high performance analysis of amino acid composition and chirality. The core processor is a four-layer microfluidic chip that performs CE separations and analyses. We have previously demonstrated MOA analysis of amino acids and their chirality,[24] bioamines, and nucleobases[25] and have analyzed a variety of Martian analogue samples with high sensitivity.[26] Successful field tests of the MOA have been conducted in the Panoche Valley, California,[26] and in the Atacama Desert, Chile.[27] Recent work using improved fluorescence labeling reagents has increased our ability to detect amines and amino acids to <10 cells per gram of soil.[28] However, since the organic carbon found on Mars could be in the form of PAHs we also need the capability to detect these compounds and their derivatives.

In this study we have extended the original MOA amino acid analysis system to the CE separation and analysis of PAHs. To perform separations of hydrophobic PAHs in aqueous solutions, we adapted a previous separation method to the microchip CE format.[16,29−31] This method employs an aqueous charge-neutral cyclodextrin as a solubilizing agent for the PAHs. A negatively charged cyclodextrin, moving against electroosmotic flow, serves as a pseudostationary phase so that the PAH separation is achieved via differential partitioning between the charged pseudostationary and the uncharged mobile cyclodextrin phases. The cyclodextrin ratio, buffer, and temperature conditions are optimized for CE based PAH separations. A standard composed primarily of PAHs found in extraterrestrial matter is used to determine limits of detection for PAHs. Finally, we apply this method to the analysis of environmental and Martian analogue samples, to evaluate the real-world utility of this analytical technique.

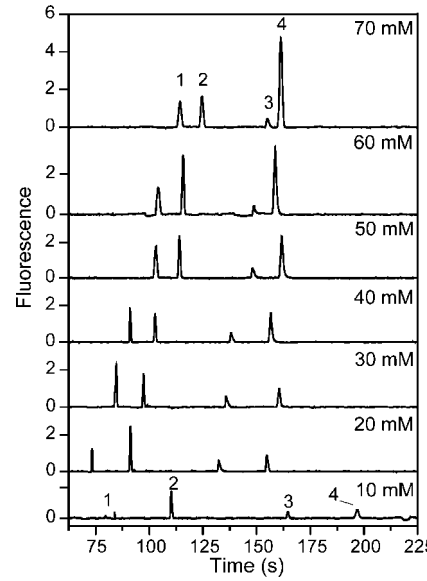

Figure 1. Dependence of PAH separation on the concentration of M-β-CD. Each sample contains 9,10-diphenylanthracene (1, 33 μM), anthracene (2, 500 μM), fluoranthene (3, 160 μM), and perylene (4, 17 μM). In addition to the indicated concentration of M-β-CD, the running buffer contains 10 mM SB-β-CD, 5 mM carbonate buffer, pH 10.

MATERIALS AND METHODS

Buffer and Sample Preparation. Methyl-β-cyclodextrin (M-β-CD) with a mean degree of substitution (ds) per cyclodextrin of 1.6−2.0 was obtained from TCI America (M1356; Portland, OR). Sulfobutylether-β-cyclodextrin (SB-β-CD) with a mean ds per cyclodextrin of 5.5 was obtained under the label Advasep 4 from Cydex, Inc. (AR-04A; Lenexa, KS). Hydroxypropyl-β-cyclodextrin (HP-β-CD, 389145) with a mean ds of 1.0 and sulfated-β-cyclodextrin (S-β-CD, 38915−3) with a mean ds of 7−11 were obtained from Sigma-Aldrich (St. Louis, MO). Stock solutions of 100 mM cyclodextrin were prepared and stored at −20 °C for up to one month. A 100 mM carbonate buffer solution was also prepared and adjusted to pH 10, then stored at room temperature. Buffers used for analysis were prepared by diluting appropriate combinations of cyclodextrin and buffer stock.

Anthracene (14106−2), fluoranthene (F807), perylene (77340), 9,10-diphenylanthracene (42785), and benzo[a]pyrene (B1760) were obtained from Sigma-Aldrich. Anthanthrene (BCR-091), benzo[ghi]fluoranthene (BCR-139), and benzo[j]fluoranthene (BCR-049) were obtained as the Community Bureau of Reference (BCR)

(19) Grundl, T. J.; Aldstadt, J. H., III; Harb, J. G.; St. Germain, R. W.; Schweitzer, R. C. *Environ. Sci. Technol.* **2003**, *37*, 1189–1197.
(20) Considine, T.; Albert, R., Jr. *Environ. Sci. Technol.* **2008**, *42*, 1213–1220.
(21) Mao, C.; McGill, K. E.; Tucker, S. A. *J. Sep. Sci.* **2004**, *27*, 991–996.
(22) Kminek, G.; Bada, J. L. *Earth Planet. Sci. Lett.* **2006**, *245*, 1–5.
(23) Aubrey, A. D.; Chalmers, J. H.; Bada, J. L.; Grunthaner, F. J.; Amashukeli, X.; Willis, P. A.; Skelley, A. M.; Mathies, R. A.; Quinn, R. C.; Zent, A. P.; Ehrenfreund, P.; Amundson, R.; Glavin, D. P.; Botta, O.; Barron, L.; Blaney, D. L.; Clark, B. C.; Coleman, M.; Hofmann, B. A.; Josset, J.-L.; Rettberg, P.; Ride, S.; Robert, F.; Sephton, M. A.; Yen, A. *Astrobiology* **2008**, *8*, 583–595.
(24) Skelley, A. M.; Mathies, R. A. *J. Chromatogr. A* **2003**, *1021*, 191–199.
(25) Skelley, A. M.; Cleaves, H. J.; Jayarajah, C. N.; Bada, J. L.; Mathies, R. A. *Astrobiology* **2006**, *6*, 824–837.
(26) Skelley, A. M.; Scherer, J. R.; Aubrey, A. D.; Grover, W. H.; Ivester, R. H. C.; Ehrenfreund, P.; Grunthaner, F. J.; Bada, J. L.; Mathies, R. A. *Proc. Natl. Acad. Sci. U.S.A.* **2005**, *102*, 1041–1046.
(27) Skelley, A. M.; Aubrey, A. D.; Willis, P. A.; Amashukeli, X.; Ehrenfreund, P.; Bada, J. L.; Grunthaner, F. J.; Mathies, R. A. *J. Geophys. Res.* **2007**, *112*, G04S11.
(28) Chiesl, T. C.; Chu, W. K.; Stockton, A.; Amashukeli, X.; Grunthaner, F.; Mathies, R. A. Submitted to *Anal. Chem.*
(29) Szolar, O. H. J.; Brown, R. S.; Luong, J. H. T. *Anal. Chem.* **1995**, *67*, 3004–3010.
(30) Nguyen, A.-L.; Luong, J. H. T. *Electrophoresis.* **1997**, *18*, 247–252.
(31) Nguyen, A.-L.; Luong, J. H. T. *Anal. Chem.* **1997**, *69*, 1726–1731.

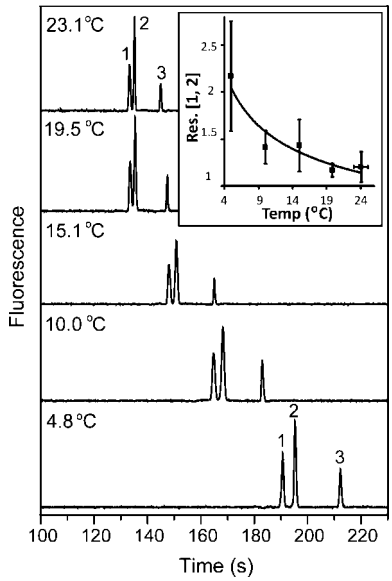

Figure 2. Dependence of PAH separation on temperature. Sample contains 9,10-diphenylanthracene (1, 1.2 μM), dibenzo[b,def]chrysene (2, 600 nM), and anthracene (3, 24 μM). Running buffer contains 10 mM SB-β-CD, 50 mM M-β-CD, 5 mM carbonate buffer, pH 10. Each data point represents the average of triplicate experiments; the error bars are calculated from the standard deviation of those experiments.

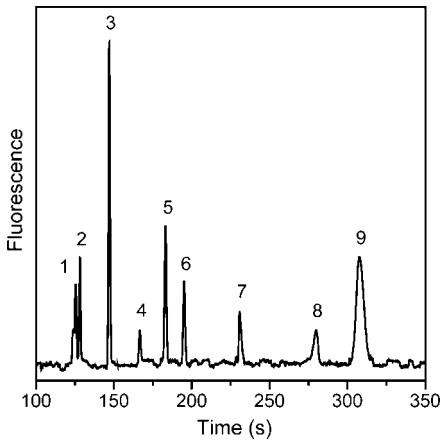

Figure 3. Separation of the Mars 9 PAH Standard (M9PAH), consisting of 9,10-diphenylanthracene (1, 800 nM), dibenzo[b,def]chrysene (2, 200 nM), anthracene (3, 300 μM), anthanthrene (4, 20 nM), benzo[a]pyrene (5, 1 μM), benzo[j]fluoranthene (6, 4 μM), fluoranthene (7, 20 μM), perylene (8, 20 nM), and benzo[ghi]fluoranthene (9, 2.5 μM). Running buffer contains 10 mM SB-β-CD, 40 mM M-β-CD, 5 mM carbonate buffer, pH 10, 20 °C.

reference materials through Sigma-Aldrich. Dibenzo[b,def]chrysene was obtained from TCI America (D1005; Portland, OR). All PAHs were used as received. Concentrated stock solutions of PAHs were prepared in electrophoresis grade acetonitrile (MeCN) or dimethylsulfoxide (DMSO) in the 50 μM to 10 mM range depending on the solubilities and optical properties. Sample stock solutions 20−100 times more concentrated than the desired final sample concentration were prepared by combining appropriate volumes of PAH stock solutions and diluting with MeCN. The final sample was prepared by diluting the stock solutions with analysis buffer to a final organic solvent composition of 1−5%.

Limits of detection (LODs) for PAHs were determined using two injection techniques: the standard cross injection and a 10 s gated injection. Each molar LOD was calculated from the average of triplicate experiments. Each dilution series consisted of 10 samples prepared from a high concentration solution in MeCN or DMSO, ranging over at least two decades. The LOD was determined as the extrapolation of a power law fit to a signal-to-noise ratio of 3. LOD samples were prepared in 1−5% MeCN or DMSO, 95−99% running buffer, depending on the solubility of each PAH.

Three samples of relevance to either the environmental or the astrobiological community were also analyzed. EC-6 is a certified reference sample for organic contaminants from Canada's National Water Research Institute (NWRI). This sample was collected in 1984 from Lake Erie and serves as one of the NWRI's reference sediments with the lowest levels of toxic organic contaminants. A hydrothermal vent chimney (HVC) sample collected from the Guaymas Basin, Gulf of California, was obtained by researchers at the Scripps Institution for Oceanographic Studies, La Jolla, CA.[32] Finally, a sample collected from the uppermost duracrust of the Yungay Hills region of the Atacama Desert, AT45A1,[27] provided an analogue to Martian regolith.

These samples were processed first either by subcritical water extraction[33] or by sublimation[34,35] to extract PAHs from the sample matrix. Freeze-dried subcritical water extracts (SCWE) were obtained from collaborators on the Urey project at the Jet Propulsion Laboratories, Pasadena, CA. Sublimation samples were obtained from collaborators at the Scripps Institution for Oceanographic Studies, La Jolla, CA. Both processes were conducted as previously reported.[33,35] Briefly, SCWE samples were obtained by extracting 1 g of sample with 8 mL of water at 200 °C and 17.2 MPa, and sublimation samples were obtained by heating the sample at 500 °C and collecting sublimate on a disk attached to a coldfinger. SCWE samples obtained were resuspended in 3 mL of water and extracted with 4×2 mL portions of dichloromethane. Sublimation disks obtained were rinsed 10 times with 100 μL portions of dichloromethane. In both cases, the dichloromethane portions were combined and evaporated, and the residue resuspended in 100 μL of running buffer. The hydrothermal vent chimney sample was diluted 1:5 with running buffer, the EC-6 sample was diluted 1:60 with running buffer, and the Atacama samples were run without dilution. Spiking experiments were conducted by adding 0.5 μL of a standard PAH solution in MeCN to 49.5 μL concentrated or diluted sample to identify and quantify PAHs in the sample.

Microdevice Fabrication. The microchip devices were prepared as previously described.[18,24−26] Briefly, a sacrificial layer of polysilicon is evaporatively deposited on a 10 cm borofloat wafer (Precision Glass & Optics, Santa Ana, CA). A layer of photoresist is spin-coated onto the polysilicon surface and patterned through a chrome mask using a contact aligner. The photoresist is developed, and the exposed polysilicon is removed via an SF_6 plasma etch. The glass is then etched in a buffered 49% HF

(32) Magenheim, A. J.; Gieskes, J. M. *Geochim. Cosmochim. Acta* **1992**, *56*, 2329–2338.
(33) Amashukeli, X.; Pelletier, C. C.; Kirby, J. P.; Grunthaner, F. J. *J. Geophys. Res* **2007**, *112*, G04S16.
(34) Glavin, D. P.; Bada, J. L. *Anal. Chem.* **1998**, *70*, 3119–3122.
(35) Kminek, G.; Bada, J. L.; Botta, O.; Glavin, D. P.; Grunthaner, F. *Planet. Space Sci.* **2000**, *48*, 1087–1091.

Table 1. Separation Characteristics of PAHs with the Mars Organic Analyzer[a]

PAH	peak no.	conc. (μM)	peak efficiency (plates per m)	res.	limits of detection[b,c] cross injection	limits of detection[b,c] 10 s gated injection	sources
9,10-diphenylanthracene	1	0.8	2.7×10^5	NA	4.4 ± 0.9 nM (150 ± 30 ppb)	2.3 ± 0.3 nM (80 ± 10 ppb)	none in literature
Dibenzo[b,def]chrysene	2	0.2	4.1×10^5	1.2	1.9 ± 0.6 nM (60 ± 20 ppb)	800 ± 200 pM (24 ± 3 ppb)	none in literature
Anthracene	3	300	4.9×10^5	8.5	100 ± 100 μM (2000 ± 2000 ppm)	20 ± 20 μM (400 ± 400 ppm)	non-Martian meteorites
Anthanthrene	4	0.02	4.1×10^5	8.0	2 ± 1 nM (60 ± 30 ppb)	1.1 ± 0.5 nM (30 ± 10 ppb)	Martian and other meteorites
Benzo[a]pyrene	5	1	5.1×10^5	6.1	5 ± 4 nM (130 ± 100 ppb)	3.2 ± 0.8 nM (80 ± 20 ppb)	Martian and other meteorites
Benzo[j]fluoranthene	6	4	5.3×10^5	4.3	150 ± 20 nM (3.8 ± 0.5 ppm)	50 ± 10 nM (1.3 ± 0.3 ppm)	Martian and other meteorites
Fluoranthene	7	20	1.7×10^5	10	500 ± 200 nM (10 ± 4 ppm)	60 ± 9 nM (1.2 ± 0.2 ppm)	Martian and other meteorites
Perylene	8	0.02	1.6×10^5	8.7	290 ± 40 pM (7 ± 1 ppb)	260 pM (6.6 ppb)	Martian and other meteorites
Benzo[ghi]fluoranthene	9	2.5	8.4 × 104	3.1	1.7 ± 0.9 μM (40 ± 20 ppm)	800 ± 300 nM (18 ± 7 ppm)	Martian and other meteorites

[a] Separation shown in Figure 3. [b] Molar limit of detection and uncertainty calculated from triplicate 10-sample experiments. [c] Parts per million/billion limit of detection calculated assuming 100% PAH recovery from 1 g soil dissolved in 100 μL running buffer.

bath for 3 min. The pattern provides 23.6 cm long folded separation channels 100 μm wide etched 25 μm deep, with a 1.2 cm long cross-channel located 0.6 cm from the anode end of the channel. The remaining photoresist is removed, and reservoir holes are drilled using 1.2 mm diamond-tipped drill bits. The polysilicon layer is removed via plasma etch, and the wafer is bonded to a blank wafer to form completed channels. A 3 mm deep PDMS gasket with 4 mm diameter wells is placed over the reservoir holes to allow for larger volume storage at the reservoirs. A schematic of the microdevice design will be found in the Supporting Information.

Mars Organic Analyzer. The Mars Organic Analyzer[25−27] was used with modifications to perform the PAH CE separations. The 404 nm laser is passed through a dichroic (Z405tranDCXR, Chroma, Rockingham, VT) and focused to a 10−20 μm spot in the channel approximately 0.6 cm from the cathode reservoir. Fluorescence is collected by the objective and reflected by the dichroic through a long pass filter (50% T at 425 nm, HQ425lp, Chroma, Rockingham, VT) onto a PMT, which was read at 50 Hz using LabView on an IBM ThinkPad laptop.

Separation and Injection Procedures. The microchip separation channel was prepared by first filling the sample, waste, and anode wells with running buffer. A vacuum was applied to the cathode well, drawing running buffer into the separation channel, and filling it with buffer. The cathode well was then filled with running buffer, and the buffer in the sample well was drawn out and replaced with sample.

Two injection techniques were used in this study. The standard cross injection was accomplished by first applying a potential across the sample (ground) and waste (−750 V) wells for 45 s, thus filling the cross channel. The anode is floated for this step, and the cathode grounded. The potentials are then switched so that the main potential is applied across the anode (ground) and cathode (−15 kV) wells. A back bias of −1200 V is applied at the sample and waste wells. The gated injection, which gives a longer sample plug, is performed by first filling the cross channel by applying −750 V at the waste, floating the anode, and grounding the sample and cathode for 45 s. Then a sample plug is injected into the column by applying −750 V at the waste, floating the anode, grounding the sample, and applying −15 kV at the cathode for 10 s. After the injection, the cathode remains at −15 kV, the anode is grounded, and a back-bias of −1200 V is again applied at the sample and waste wells.

Safety. Several PAHs have been identified as or are suspected of being carcinogens. PAH solids and stock solutions were handled in a ventilated hood and stored in closed containers. Disposable nitrile gloves were worn while working with PAHs.

RESULTS AND DISCUSSION

Effect of Charged Cyclodextrin on PAH Separations. To explore the dependence of PAH separation quality on the identity and concentration of the charged CD, sulfated-β-cyclodextrin (S-β-CD) and sulfobutylether-β-cyclodextrin (SB-β-CD) were used in varying concentrations in a constant 40 mM methyl-β-cyclodextrin (M-β-CD), 5 mM carbonate buffer, pH 10. The sample containing 40 μM 9,10-diphenylanthracene, 600 μM anthracene, and 20 μM perylene in 5% MeCN, 95% running buffer was injected via a cross-injection. No separation was observed at any concentration of S-β-CD. Supporting Information, Figure S2 presents electropherograms of PAH separations at concentrations of SB-β-CD varying from 0 to 10 mM. With no SB-β-CD, there is no separation of PAH components, and they emerge as a single peak. This is expected, since all PAHs elute with the mobile M-β-CD phase. As the concentration of SB-β-CD is increased, PAH separation is accomplished and average migration time is increased. This migration time increase is due to enhanced partitioning of the PAHs into the negatively charged SB-β-CD at higher concentrations of this CD. Larger SB-β-CD concentrations also increase the signal-to-noise ratio because more PAHs are solubilized. The highest resolution and signal-to-noise was observed at the highest 10 mM concentration of SB-β-CD. Increasing the SB-β-CD concentration also increased currents during the separation, which imposed a maximum practical limit to the SB-β-CD concentration

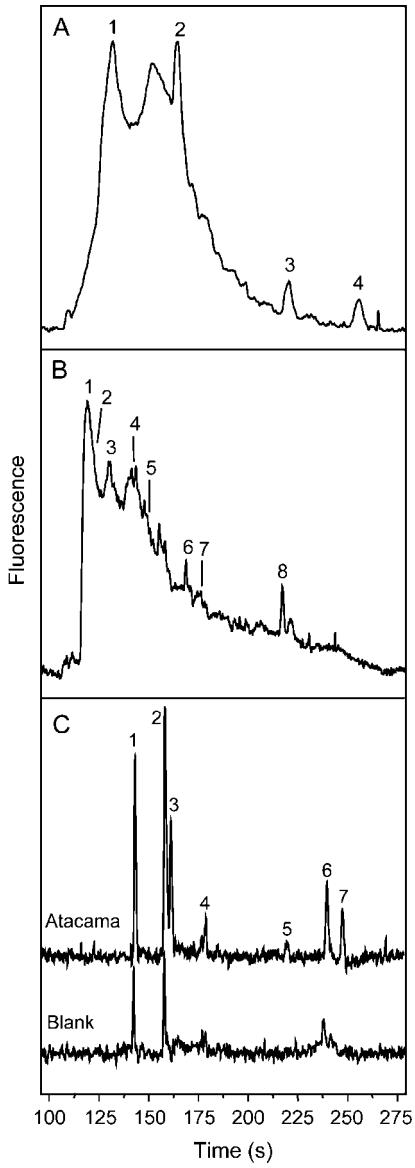

Figure 4. Analysis of complex real-world samples for PAHs. (A) Separation of a subcritical water extract of NWRI certified reference sediment EC-6 from Lake Erie, (B) a sublimed component of a hydrothermal vent chimney (HVC), and (C) a subcritical water extract of Atacama duracrust surface sample AT45A1. PAHs in the EC-6 sample are anthracene (1, 118 ± 9 ppb), benzo[a]pyrene (2, 20 ± 10 ppb), fluoranthene (3, 831 ± 10 ppb), and benzo[ghi]fluoranthene (4, 86 ± 1 ppb). PAHs identified in the HVC sample include 9,10-diphenylanthracene (1), dibenzo[b,def]chrysene (2), anthracene (3), pentacene (4), anthanthrene (5), benzo[a]pyrene (6), benzo[j]fluoranthene (7), and fluoranthene (8). The Atacama sample was taken from the top 1 cm of duracrust in the Yungay Hills region of the Atacama Desert, Chile.[25] PAH quantities in the sample adjusted for blank composition are 400 ± 100 ppb 9,10-diphenylanthracene (1, 920 ± 20 ppb Blank), 9000 ± 6000 ppm anthracene (3), 180 ± 80 ppb anthanthrene (4, 150 ± 60 ppb Blank), 400 ± 300 ppb fluoranthene, 2 ± 1 ppb perylene (6, 3 ± 1 ppb Blank), and 70 ± 50 ppm benzo[ghi]fluoranthene (7). The blank is a subcritical water flush of the extraction system between samples.

at ~10 mM and ~100 μA. Above this concentration, electrolysis and bubble formation led to separation failures.

Effect of Neutral Cyclodextrin on PAH Separations. To choose the optimal neutral CD and concentration, two uncharged cyclodextrins, M-β-CD and hydroxypropyl β cyclodextrin (HP-β-CD), were used in varying amounts in a constant 10 mM SB-β-CD, 5 mM carbonate buffer, pH 10 (Figure 2). The sample containing 9,10-diphenylanthracene, anthracene, fluoranthene, and perylene in 5% MeCN, 95% running buffer was cross-injected. Separations using HP-β-CD (results not shown) produced coelution of 9,10-diphenylanthracene and anthracene peaks at some concentrations of HP-β-CD and overall lower resolution than M-β-CD, so this combination was not explored further. Figure 1 shows electropherograms of PAH separations at concentrations of M-β-CD varying from 10 to 70 mM. Higher resolution between peaks and an overall average longer migration time is observed at lower concentrations of M-β-CD, while higher signal strength and hence signal-to-noise ratios are observed at higher concentrations of M-β-CD. The resolution between the anthracene and the fluoranthene peaks and between the fluoranthene and the perylene peaks is plotted in Supporting Information, Figure S3 at the concentrations of M-β-CD tested, and a general downward trend in resolution with increasing M-β-CD is seen. This trend is expected, since as the concentration of M-β-CD is increased, PAHs become more likely to associate with M-β-CD over SB-β-CD; thus, the effectiveness of the pseudostationary phase is decreased. Signal-to-noise ratios for anthracene and perylene are also plotted, and a general upward trend in signal-to-noise ratio with increasing M-β-CD is seen. This trend is due to the increased total PAH concentration that can be solubilized in higher total CD concentration. The crossing point of these two trends occurs at approximately 40 mM M-β-CD. The cyclodextrin mixture chosen for further parameter optimization was 10 mM SB-β-CD and 50 mM M-β-CD to give better signal strength of all PAH peaks during optimization experiments while showing similar separation characteristics to the optimal 40 mM M-β-CD.

Effect of Temperature on PAH Separation. Many parameters were examined for their effects on the PAH separation, including separation field strength, injection parameters, addition of organic solvents, carbonate buffer concentration, and temperature. The only parameter to show desirable effects on separation was temperature. Samples containing 1.2 μM 9,10-diphenylanthracene, 600 nM dibenzo[b,ef]chrysene, and 24 μM anthracene in 5% MeCN, 95% running buffer were cross injected. Figure 2 presents electropherograms of the PAH separations at temperatures from 5 °C (bottom) to room temperature (top) in 5 °C increments. At room temperature (~23 °C), all peaks emerge after about 120 s, and the 9,10-diphenylanthracene and dibenzo[b,def]chrysene peaks are quite close (resolution ≈ 1). At about 5 °C, the retention times are increased, and there is significantly increased resolution between all three peaks. This trend is shown in the inset (top right), which plots the resolution between the 9,10-diphenylanthracene and the dibenzo[b,def]chrysene peaks at each temperature tested. The data show a clear increase in resolution at 5 °C but relatively similar resolution at 10 °C and higher. At temperatures less than about 15 °C, however, late-migrating PAHs such as fluoranthene, perylene, and benzo[ghi]fluoranthene occasionally fail to elute (not shown). The current Urey operation protocol calls for regulation of the chip separation temperature at 4 °C.

Separation of the Mars 9 PAH Standard. Figure 3 presents an electropherogram of the separation of the Mars 9 PAH standard (M9PAH). The PAHs in this standard were chosen based on their

Table 2. PAH Analysis of Environmental and Martian Analogue Samples[a]

PAH	hydrothermal vent chimney[b]	EC-6 (NWRI)[c]	EC-6 (MOA)[d]	Atacama Blank[d]	Atacama sample (above Blank)[d]
9,10-diphenylanthracene	7 (−2) − 17 (+3) ppb[e]			920 ± 20 ppb	400 ± 100 ppb
Dibenzo[b,def]chrysene	0.12 (−0.04) − 5 (+2) ppb				
Anthracene	50 (−50) − 100 (+100) ppb	37 ppb	118 ± 9 ppb		9000 ± 6000 ppm
Pentacene					
Anthanthrene	0.3 (−0.3) − 4 (+2) ppb			150 ± 60 ppb	180 ± 80 ppb
Benzo[a]pyrene	2 (−2) − 6 (+6) ppb	250 ppb	20 ± 10 ppb		
Benzo[j]fluoranthene	200 (−100) − 1000 (+400) ppb				
Fluoranthene	220 (−70) − 400 (+100) ppb	297 ppb	831 ± 10 ppb		400 ± 300 ppb
Perylene				3 ± 1 ppb	2 ± 1 ppb
Benzo[ghi]fluoranthene		175 ppb	86 ± 1 ppb		70 ± 50 ppm

[a] Composition calculated for initial sample assuming 100% recovery during subcritical water and dichloromethane extraction. [b] Analysis conducted of dichloromethane soluble portion of sublimate. [c] Non-certified values as quoted by the National Water Research Institute, Environment Canada, Burlington, Ontario, CA. [d] Analysis conducted of dichloromethane soluble portion of SCWE. [e] Ranges determined by assuming no baseline obscuring of peak for the lower value and no baseline contribution to peak for the larger value. Errors are calculated for each assumption to give the ranges and errors listed.

optical properties, specifically absorbance at 404 nm, and their presence in extraterrestrial matter. Seven of the PAHs in the standard are found in significant amounts in extraterrestrial matter, including Martian and non-Martian meteorites, while the remaining two PAHs are found predominantly as terrestrial contaminants. M9PAH was injected via a cross injection in 5% MeCN, 95% running buffer. The concentrations of PAHs used in this separation range from 20 nM for anthanthrene and perylene to 300 μM for anthracene. Average peak efficiency for this separation is around 3×10^5 plates per meter, and the high resolutions (>1) reflect the lack of overlapping peaks. The concentrations, identities, and sources of PAHs in this standard are given in Table 1, along with the characterization of this separation, including the peak efficiencies and resolutions.

Limits of Detection. Limits of detection (LODs) for the studied PAHs are listed in Table 1. Cross injection LODs range from 100 μM (2 parts per thousand) for anthracene down to 290 pM (7 ppb) for perylene. Gated injection LODs are around one tenth to one half those determined using the cross injection and range from 20 μM (400 ppm) for anthracene to 260 pM (6 ppb) for perylene. These LODs are dependent on individual PAH spectral properties and would be expected to improve upon transitioning to a shorter-wavelength excitation laser. Also, because of competitive and cooperative binding effects that occur when there are multiple PAHs in solution, these LODs may not be representative of true detection limits in a complex mixture. The signal for anthracene, in particular, is extremely sensitive to the presence of other PAHs. Although its calculated LOD is in the hundreds of μM range, it is easily detectable at lower concentrations if other PAHs are present. For example, the anthracene signals in Figure 2 are quite strong despite its only 24 μM concentration. However, perylene, which has a LOD in the hundreds of pM range, shows a relatively weak signal in Figure 3 at 20 nM. These effects are likely due to competitive and cooperative binding, respectively. Despite these effects, these LOD results indicate the usefulness of this method for highly sensitive in situ PAH detection.

Complex Samples. To validate the MOA for the detection and separation of PAHs, a number of samples of environmental and astrobiological interest were examined. Figure 4A shows the analysis of a SCWE of EC-6, Canada's National Water Research Institute's (NWRI's) sediment standard for low level PAH contamination. The peaks corresponding to the PAH contaminants anthracene (3), benzo[a]pyrene (6), fluoranthene (8), and benzo[ghi]fluoranthene (9) are readily observed and identified via spiking experiments. This identification agreed with that determined by NWRI laboratories, according to NWRI product literature. Quantification yields sediment contamination of 118 ± 9, 20 ± 10, 831 ± 10, and 86 ± 1 ppb for anthracene, benzo[a]pyrene, fluoranthene, and benzo[ghi]fluoranthene, respectively, as compared to the NWRI values of 37, 250, 297, and 175 ppb. These results are summarized in Table 2. The MOA-determined values are 3 to 12-fold lower than those determined by the NWRI for benzo[a]pyrene and for benzo[ghi]fluoranthene. This difference is most likely due to the SCWE protocol, which was optimized for amino acid extraction with a subcritical water dielectric constant of ~35. Since PAHs are more hydrophobic than amino acids, extraction efficiency of these molecules would be expected to dramatically increase upon raising the temperature of the SCWE to produce dielectric constants <15.[33] The MOA-determined values for anthracene and fluoranthene are larger than the NWRI values by a factor of approximately three. According to NWRI product literature, the sample contains PAHs and PCBs invisible to the 404 nm detection system. The cooperative binding effect of PAHs to cyclodextrins noticed during the determination of the limits of detection may account for the three-fold enhancement.

Figure 4B presents the analysis of a sublimate of a hydrothermal chimney vent from the Guaymas Basin, Gulf of California.[32] Peaks are seen for a number of components, including 9,10-diphenylanthracene dibenzo[b,def]chrysene, anthracene, pentacene, anthanthrene, benzo[a]pyrene, benzo[j]fluoranthene, and fluoranthene. While the total PAH concentration in this sample is large, the number of components makes quantification of the concentration of a single component difficult because of the strong background signal. Because of these difficulties, ranges of PAH concentrations are estimated and are listed in Table 2. The maximum concentration was determined by using the baseline-to-peak height to determine the PAH signal (i.e., no non-PAH background contribution to detected signal), the minimum was determined by subtracting the large background profile to expose only the PAH spikes (i.e., no PAH signal buried in background). A large concentration and variety of PAHs is expected in HVCs, and our results agree with those published in other HVC samples.[11]

Figure 4c presents the analysis of the SCWE of sample AT45A1[27] from the top 1 cm of the duracrust in the Yungay Hills region of the Atacama Desert (Atacama) compared to a subcritical water system flush (Blank). Six PAH components are found in this sample, including 9,10-diphenylanthracene (400 ± 100 ppb), anthracene (9000 ± 6000 ppm), anthanthrene (180 ± 80 ppb), fluoranthene (400 ± 300 ppb), perylene (2 ± 1 ppb above background), and benzo[ghi]fluoranthene (70 ± 50 ppm). PAHs in the blank system flush include 9,10-diphenylanthracene (920 ± 20 ppb), anthanthrene (150 ± 60 ppb), and perylene (3 ± 1 ppb), and are probably due to system carryover between samples. These results are summarized in Table 2. While there is little information on PAHs in the Yungay Hills region in the literature, the total organic matter has been cited in the 20−40 ppm range.[36] Despite using spiking experiments to calibrate, the quantization of anthracene is not consistent with either this result or the low levels of other PAHs in the sample and is probably an overestimate due to cooperative binding effects. The Yungay Hills region of the Atacama Desert is the driest in the world, receiving only one significant rain event of 2.3 mm over a four year observation period.[37] Because of the perpetually dry conditions and prolonged UV exposure on the surface of this 1 million year old desert, the Atacama duracrust serves as the best possible terrestrial model for soil conditions and composition and amounts of organic molecules on the Martian surface. The success of the MOA in detecting and analyzing PAHs in this sample indicates that the MOA is technically competent to detect PAHs on or below the Martian surface if they are present.

CONCLUDING REMARKS

The method for PAH analysis developed here significantly advances the capabilities of the MOA for organic carbon detection and may also prove useful for environmental monitoring. This method exploits a mixture of charged and uncharged CDs to solubilize and mobilize the hydrophobic PAHs in an aqueous solution for convenient CE analysis without organic solvents. Resolutions >1 are achieved between PAHs of the same molecular weight and of similar structures. Excellent limits of detection are observed for some PAHs, down to 7 ppb or 260 pM, which is comparable to other currently used laboratory methods. We have demonstrated the utility of this method for the analysis of samples of interest to the environmental community and to the astrobiology community with the analysis of the Mars analogue sample from the Atacama Desert.

Improvements to the MOA analysis system to enable the detection of additional PAHs are also possible. On the basis of the absorbance spectra of PAHs found in extraterrestrial sources, the number of detectable PAHs could be expanded by moving to a shorter wavelength excitation laser. Meteoric PAHs pyrene, benzo[ghi]perylene, and coronene are undetectable with the 404 nm detection system but would be detectable on a system that uses a 350 nm excitation laser. Excitation at 350 nm would also significantly increase the sensitivity of the MOA for many of the PAHs observed with the current system. Even shorter wavelength lasers may enable the detection of the highly oxidized mellitic acid[10] as well. For more details on the development of the MOA for planetary exploration, see http://astrobiology.berkeley.edu.

ACKNOWLEDGMENT

We thank the Urey Instrument team for support and comments, and especially Xenia Amashukeli for providing SCWE samples, Andrew Aubrey for providing sublimation samples, and Pascale Ehrenfreund for informative discussion. Microdevices were constructed in the Berkeley Microfabrication Laboratory by Eric Chu. This research was supported by NASA Grant NNX08AR09G and by Jet Propulsion Laboratory Contract No. 1297596.

SUPPORTING INFORMATION AVAILABLE

Further details are given in Figures S1−S3. This material is available free of charge via the Internet at http://pubs.acs.org.

Received for review September 24, 2008. Accepted November 13, 2008.

AC802033U

(36) Navarro-Gonzalez, R.; Navarro, K. F.; de la Rosa, J.; Iniguez, E.; Molina, P.; Miranda, L. D.; Morales, P.; Cienfuegos, E.; Coll, P.; Raulin, F.; Amils, R.; McKay, D. S. *Proc. Natl. Acad. Sci. U.S.A.* **2006**, *103*, 16089–16094.

(37) McKay, D. S.; Friedmann, B.; Gomez-Silva, B.; Cacerces, L.; Andersen, D. T.; Landheim, R. *Astrobiology* **2003**, *3*, 393–406.